Available online at www.sciencedirect.com
ScienceDirect
Trans. Nonferrous Met. Soc. China 25(2015) 2893−2900
Transactions of Nonferrous Metals Society of China
www.tnmsc.cn

Microstructure and mechanical properties of heat-treated Ti−5Al−2Sn−2Zr−4Mo−4Cr

Hui-min LI, Miao-quan LI, Jiao LUO, Ke WANG

School of Materials Science and Engineering, Northwestern Polytechnical University, Xi'an 710072, China

Received 9 October 2014; accepted 25 March 2015

Abstract: The effects of heat treatment parameters on the microstructure, and mechanical properties and fractured morphology of Ti−5Al−2Sn−2Zr−4Mo−4Cr with the equiaxed, bi-modal and Widmanstätten microstructures were investigated. The heating temperatures for obtaining the equiaxed, bi-modal and Widmanstätten microstructures were 830, 890 and 920 °C, respectively, followed by furnace cooling at a holding time of 30 min. The volume fraction of primary α phase decreased with increasing the heating temperature, which was 45.8% at 830 °C, and decreased to 15.5% at 890 °C, and then the primary α phase disappeared at 920 °C during furnace cooling. The variation of volume fraction of primary α phase in air cooling is similar to that in furnace cooling. The increase in heating temperature and furnace cooling benefited the precipitation and growth of the secondary α phase. The equiaxed microstructure exhibited excellent mechanical properties, in which the ultimate strength, yield strength, elongation and reduction in area were 1035 MPa, 1011 MPa, 20.8% and 58.7%, respectively. The yield strength and elongation for the bi-modal microstructure were slightly lower than those of the equiaxed microstructure. The Widmanstätten microstructure exhibited poor ductility and low yield strength, while the ultimate strength reached 1078 MPa. The dimple fractured mechanism for the equiaxed and bi-modal microstructures proved excellent ductility. The coexistence of dimple and intercrystalline fractured mechanisms for the Widmanstätten microstructure resulted in the poor ductility.

Key words: titanium alloy; heat treatment; microstructure; mechanical properties; fractured morphology

1 Introduction

The mechanical properties of titanium alloys are sensitive to the microstructure, including volume fraction, grain size and distribution of α and β phases [1−3]. MARKOVSKYA and SEMIATIN [4] pointed out that the formation of substructure, martensite, and residual stress in CP-Ti influenced the strength and fatigue behavior. SIENIAWSKI et al [5] proposed that the stable β phase after heat treatment improved the mechanical properties of Ti−6Al−2Mo−2Cr. The reduced slip length between the secondary lamellar α phase significantly affected the proof stress, yield stress and fracture toughness of Ti−6Al−4V and Ti−6Al−2Mo−2Cr [6,7]. LÜTJERING [8] presented that a decrease in α colony size improved the yield stress and ductility of Ti−6Al−4V and Ti−6Al−2Sn−4Zr−2Mo. SHI et al [9] found that the cooling rate in β field after annealing and the subsequent annealing on the top of α+β field determined the content and morphology of coarse α plates. FILIP et al [6] pointed out that the low cooling rate led to the diffusion-controlled growth of α phase lamellae in Ti−6Al−4V and Ti−6Al−2Mo−2Cr, and the thickness and length of the α phase decreased with the increase of cooling rate and β-stabilizing element content.

The Ti−5Al−2Sn−2Zr−4Mo−4Cr (corresponding to ASTM Ti-17 alloy) was widely used to manufacture the aerofoil blades and discs at the servicing temperature below 500 °C [10]. The volume fraction and grain size of primary and secondary α phases were determined by the heat treatment parameters [11]. Up to now, the flow stress, apparent activation energy for deformation and globularization of the primary α phase during hot deformation of Ti−5Al−2Sn−2Zr−4Mo−4Cr have been investigated [12,13]. TARÍN et al [14] studied the transformation kinetics and micrographic evaluations of Ti−5Al−2Sn−2Zr−4Mo−4Cr under different solution and aging conditions. TEIXEIRA et al [15] presented that

Foundation item: Projects (51205318, 51275416) supported by the National Natural Science Foundation of China; Project (3102014JCQ01016) supported by the Fundamental Research Funds for the Central Universities, China
Corresponding author: Miao-quan LI; Tel: +86-29-88460328; Fax: +86-29-88492642; E-mail: honeymli@nwpu.edu.cn
DOI: 10.1016/S1003-6326(15)63915-2

the Ti−5Al−2Sn−2Zr−4Mo−4Cr could retain the whole β phase at a metastable state during quick quenching, and the heat treatment parameters collaboratively controlled the microstructure.

Although a lot of researches have been done, the relationship between the typical microstructure and the mechanical properties of Ti−5Al−2Sn−2Zr−4Mo−4Cr after heat treatment has not been investigated. Therefore, in this work, the Ti−5Al−2Sn−2Zr−4Mo−4Cr was treated at different temperatures with given cooling rates, and the effects of the heat treatment parameters on the typical microstructures, including the equiaxed, bi-modal and Widmanstätten microstructures of Ti−5Al−2Sn−2Zr−4Mo−4Cr were investigated. Following choosing the optimal heat treatment parameters, the mechanical properties of Ti−5Al−2Sn− 2Zr−4Mo−4Cr with typical microstructures at room temperature were determined.

2 Experimental

2.1 Materials

The chemical composition of the as-received Ti−5Al−2Sn−2Zr−4Mo−4Cr with a diameter of 50 mm is shown in Table 1, and the β-transus temperature of the alloy is about 905 °C via metallographic method. Prior to heat treatment, isothermal annealing was performed at 840 °C for 2 h, furnace cooling to 650 °C in 2 h and then air cooling to room temperature so as to obtain the equiaxed microstructure.

Table 1 Chemical composition of as-received Ti−5Al−2Sn−2Zr−4Mo−4Cr (mass fraction, %)

Al	Sn	Zr	Mo	Cr	Fe
5.12	2.03	2.10	4.04	3.94	0.10

C	N	H	O	Ti
0.12	0.007	0.007	0.12	Bal.

2.2 Heat treatment

The dimensions of Ti−5Al−2Sn−2Zr−4Mo−4Cr samples were 5 mm × 5 mm × 8 mm. The heat treatment was carried out in a box-type resistance furnace with furnace cooling (FC) and/or air cooling (AC) at temperatures of 830, 860, 870, 880, 890 and 920 °C, respectively, and a holding time of 30 min. After heat treatment, the Ti−5Al−2Sn−2Zr−4Mo−4Cr specimens were cross-sectioned, mechanically polished using silicon carbide paper, electrolytically polished and chemically etched in a solution of 10 mL HF, 15 mL HNO_3 and 75 mL H_2O. The microstructure examination was carried out on an OLYMPUS PM−T3 optical microscope. The grain size and volume fraction of primary α phase were measured by using an Image Pro plus 6 software. The experimental values were calculated from the 12 visual fields.

2.3 Tension

Tension specimens with a gauge length of 25 mm and a diameter of 5 mm were manufactured from the heat-treated Ti−5Al−2Sn−2Zr−4Mo−4Cr bar. The tension of Ti−5Al−2Sn−2Zr−4Mo−4Cr heat-treated at room temperature was carried out on a Zwick 105 electronic universal testing machine. The ultimate strength (UTS), yield strength (YS), reduction in area (RA) and elongation (El) were the average values of three specimens. The fractured surfaces of Ti−5Al−2Sn−2Zr−4Mo−4Cr specimens after tension were observed by using a MIRA3 TESCAN scanning electron microscope at 20 kV.

3 Results and discussion

3.1 As-received microstructure

As seen from Fig. 1(a), the transversal microstructure of as-received Ti−5Al−2Sn−2Zr−4Mo−4Cr consists of the equiaxed α phase with a volume fraction of 34.9% and grain size of 3.29 μm and the β matrix. The longitudinal morphology of α phase is short rod and shows a certain orientation along the axial direction in Fig. 1(b).

3.2 As-treated microstructure

3.2.1 Effect of heating temperature

The effect of heating temperature on the

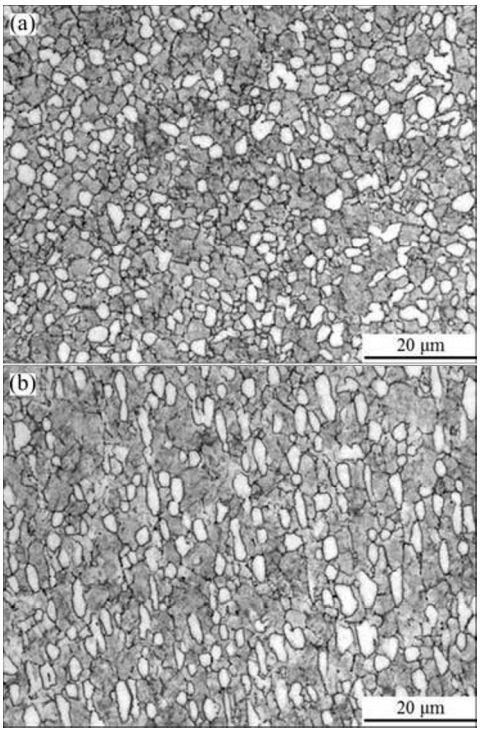

Fig. 1 Micrographs of as-received Ti−5Al−2Sn−2Zr−4Mo−4Cr specimens: (a) Transversal; (b) Longitudinal

microstructure of Ti−5Al−2Sn−2Zr−4Mo−4Cr is shown in Fig. 2. Quantitative assessment of the grain size and volume fraction of primary α phase is obtained and shown in Fig. 3.

The volume fraction of primary α phase keeps steady in the temperatures ranging from 830 to 880 °C, decreases at 890 °C (Fig. 3(a)), and disappears at 920 °C (Fig. 2(f)). At 830 °C, the volume fraction of primary α

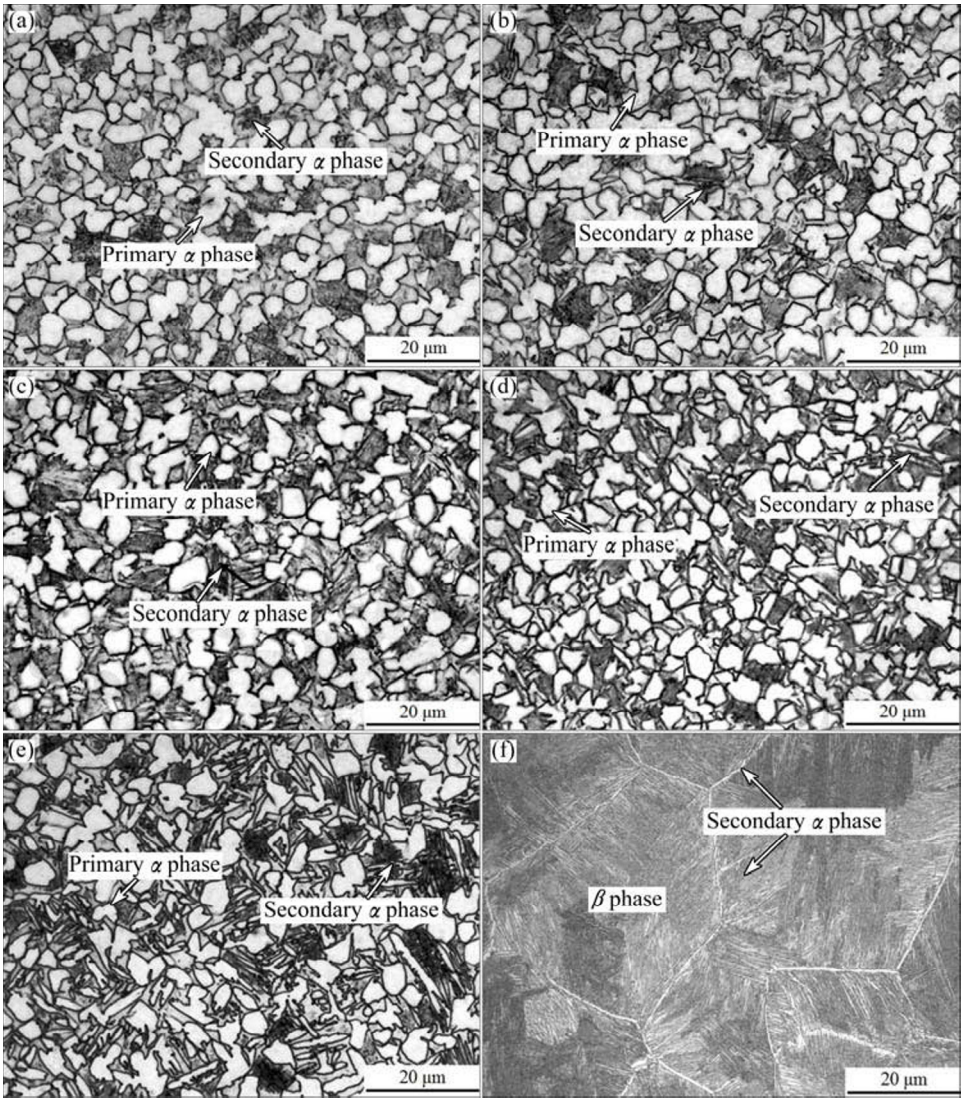

Fig. 2 Micrographs of Ti−5Al−2Sn−2Zr−4Mo−4Cr following FC at different heating temperatures: (a) 830 °C; (b) 860 °C; (c) 870 °C; (d) 880 °C; (e) 890 °C; (f) 920 °C

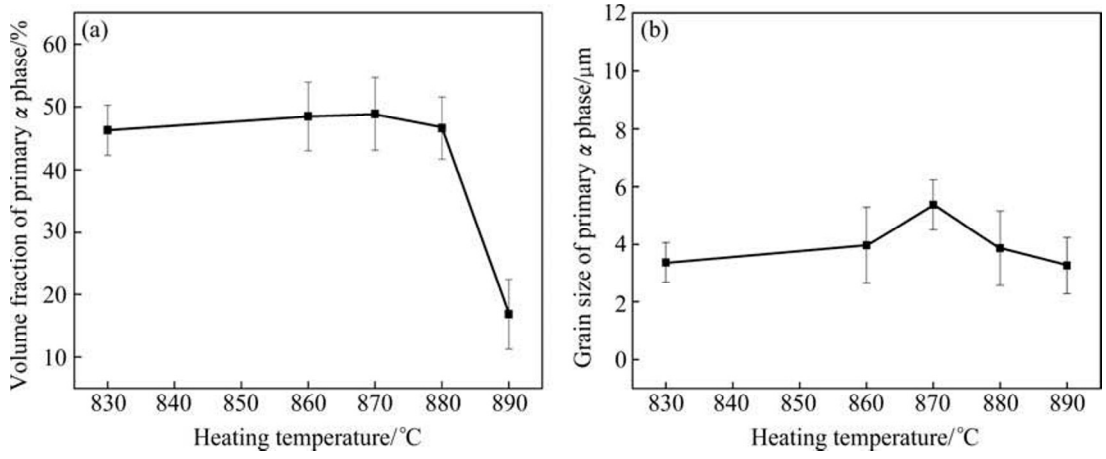

Fig. 3 Effect of heating temperature following FC on volume fraction (a) and grain size (b) of primary α phase

phase increases from 34.0% to 45.8% compared with that of the as-received sample. The FC promotes adequate transformation of $\beta \rightarrow \alpha$ and the grain size of α phase, then the volume fraction of primary α phase keeps steady at temperatures ranging from 830 to 880 °C; however, the volume fraction of primary α phase sharply decreases to 15.5% as the heating temperature increases to 890 °C.

The heating temperature has little effect on the grain size of primary α phase, which fluctuates between 3 and 5.5 μm in the temperature range of 830−890 °C, as seen in Fig. 3(b). The morphology of the secondary α phase varies with the increase of heating temperature. Small amounts of fine secondary α lamellae occur at 830 °C. Both the width and amount of the secondary α lamellae increase with the increase of heating temperature, as the amount of secondary α phase increases with prolonging cooling time [16,17].

3.2.2 Effect of cooling condition

The microstructures of Ti−5Al−2Sn−2Zr−4Mo−4Cr followed by AC at a given heating temperature and/or FC are shown in Fig. 4. As seen from Figs. 4(a), (c) and (e), the volume fraction of primary α phase decreases with the increase of heating temperature, and the secondary α phase does not occur. At a heating temperature of 830 °C (Fig. 4(a)), the grain size is 2.65 μm and volume fraction is 25.03%, and those decrease to 2.06 μm and 4.58%, respectively, as the heating temperature increases closely to β-transus temperature (Fig. 4(c)). The primary α phase of Ti−5Al−2Sn−2Zr−4Mo−4Cr at a heating temperature of 920 °C totally disappears. Low cooling rate in FC mainly affects the growth of primary α phase and the precipitation of the secondary α phase, as shown in Figs. 4(b), (d) and (f). FC promotes the diffusion of

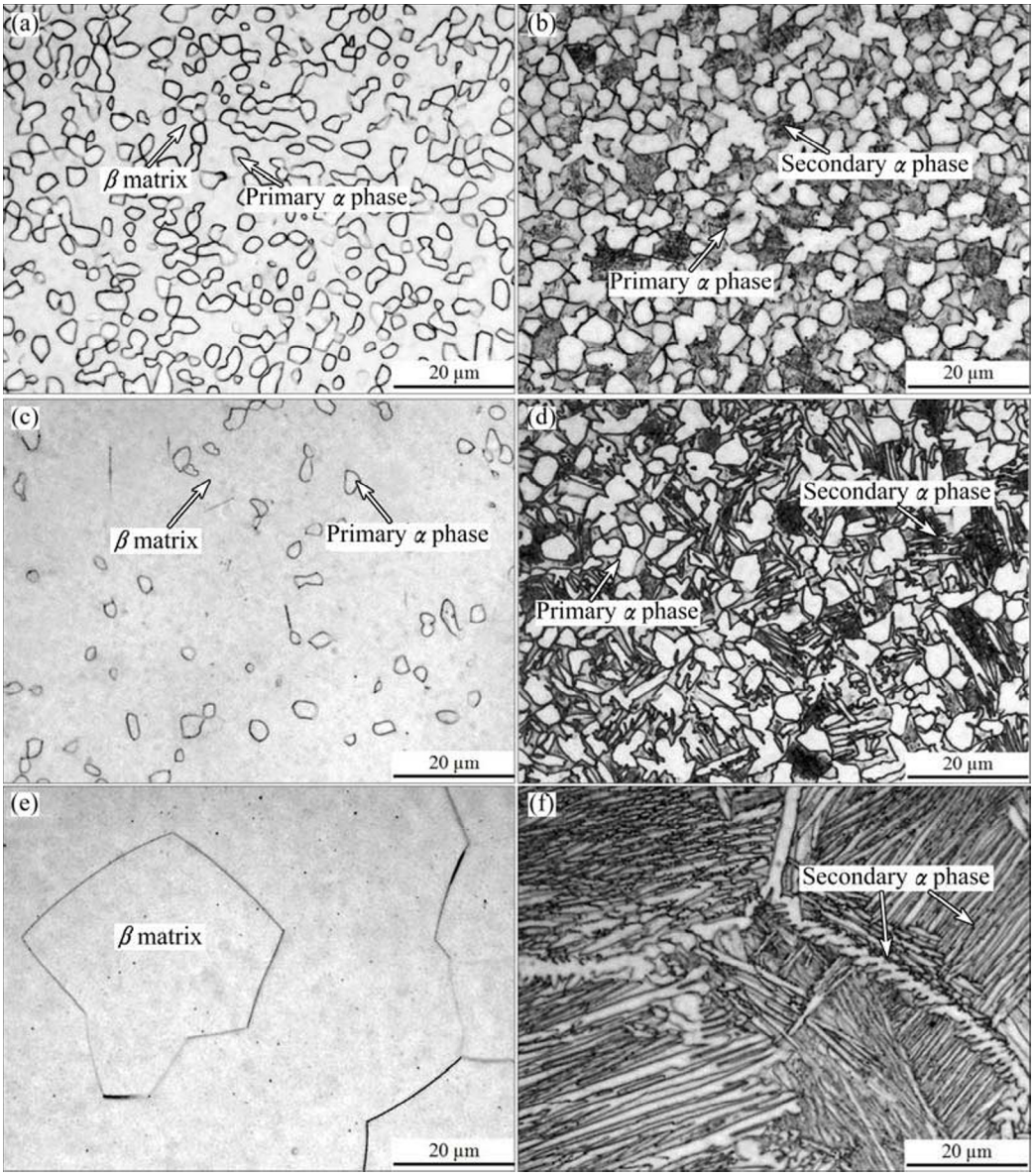

Fig. 4 Micrographs of Ti−5Al−2Sn−2Zr−4Mo−4Cr at 830 °C + AC (a), 830 °C + FC (b), 890 °C + AC (c), 890 °C + FC (d), 920 °C + AC (e) and 920 °C + FC (f)

atoms and the nucleation of secondary α phase. Comparing Figs. 4(b) and (d) with Figs. 4(a) and (c), the secondary α phase precipitates, and both volume fraction and grain size of primary α phase followed by FC increase, as obtained in Ref. [18]. Comparing Fig. 4(f) with Fig. 4(e), the interlaced arranged α colony with different directions precipitates in the coarse β matrix and α plates occur at β grain boundaries.

Based on the above discussion, the heat treatment parameters for the three typical microstructures are obtained as follows: 1) 830 °C, 30 min and FC for equiaxed microstructure, 2) 890 °C, 30 min and FC for bi-modal microstructure, and 3) 920 °C, 30 min and FC for Widmanstätten microstructure.

3.3 Mechanical properties

The variations of the UTS (σ_b), YS ($\sigma_{0.2}$), El (ε) and RA (A) with the heating temperature for three typical microstructures are depicted in Fig. 5. Both the equiaxed and bi-modal microstructures exhibit high strength and good ductility. The UTS values of equiaxed and bi-modal structures are at the same level. The YS of the equiaxed microstructure is slightly higher than that of the bi-modal microstructure. In contrast, the Widmanstätten microstructure exhibits poor ductility with low El, RA and YS, while UTS is high.

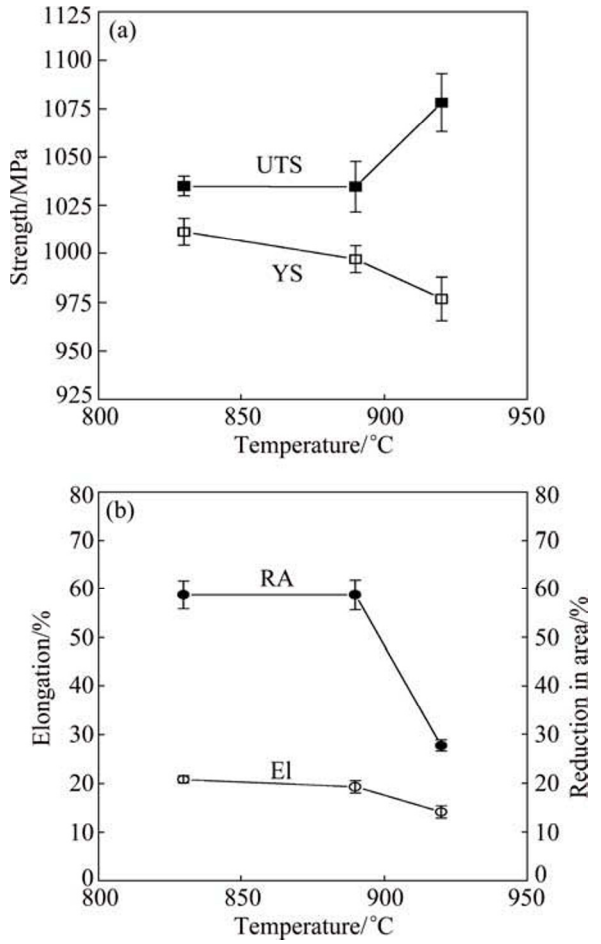

Fig. 5 Variation of UTS, YS, El and RA for three typical microstructures with heating temperature followed by FC

Three typical microstructures behave high UTS, especially for Widmanstätten microstructure. As to the equiaxed and bi-modal microstructures, the primary α phase with small grain size of 3−4 μm benefits to improve the UTS. Besides, the strengthening effect of the secondary α phase increases with the decrease of primary α phase [19]. For Widmanstätten microstructure, further increase in UTS is attributed to an increase in secondary α lamellae, which increases the total content of α phase.

The decrease in YS is closely related to incoherent boundaries between primary α phase and β phase, and semi-coherent boundaries between secondary α phase and β phase. As seen from Figs. 2(a), (e) and (f), the volume fraction of the primary α phase sharply decreases in the bi-modal microstructure, and totally disappears in the Widmanstätten microstructure. The variation of the secondary α phase is exactly opposite. Therefore, the amount of incoherent boundaries decreases while that of semi-coherent boundaries increases, then the YS decreases. Besides, the coarse β grain also decreases the YS of the Widmanstätten microstructure according to the Hall−Petch relationship. The colony-type and coarse α plates resulting from FC also decrease the YS [8,20].

Both the equiaxed and bi-modal microstructures exhibit good ductility. As to the equiaxed microstructure, large amounts of small equiaxed primary α grains and fine secondary α phase decrease the slip length. For the bi-modal microstructure, an increase in the size of secondary α phase is advantageous to the increase of ductility [21]. The Widmanstätten microstructure behaves poor ductility, in which the coarse β grains with an average grain size of 236 μm and large secondary α colonies are the main factor, and the continuously distributed boundary α lamella is another factor to decrease the ductility of Widmanstätten microstructure.

The fractured mechanisms of equiaxed, bi-modal and Widmanstätten microstructures in the room temperature tension were checked by the fractured morphologies shown in Figs. 6 and 7. As seen from Figs. 6(a) and (c), large shrinkages in both equiaxed and bi-modal microstructures occur. As seen from Figs. 6(b) and (d), deep and homogenous dimples on the fractured surfaces occur. Large shrinkage, plenty of deep and big ductile dimples on the fractured surfaces of the equiaxed and bi-modal microstructures prove good tensile properties. As seen from Fig. 7(a), little contraction in the tension of Widmanstätten microstructure occurs. As seen from Figs. 7(b) and (c), the dimple and intercrystalline fracture occur, in which the dimples are much smaller and shallower than those of the equiaxed and bi-modal microstructures so as to decrease the

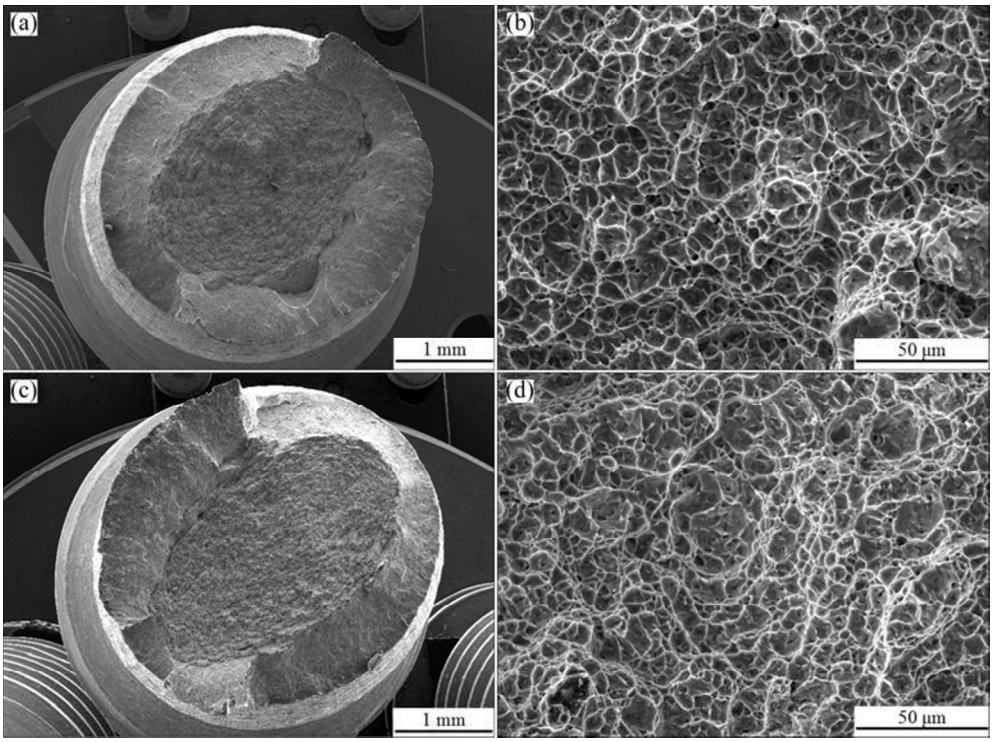

Fig. 6 Fractured morphology of heat-treated Ti−5Al−2Sn−2Zr−4Mo−4Cr specimens with equiaxed microstructure (a) and corresponding magnification image (b), and bi-modal microstructure (c) and corresponding magnification image (d)

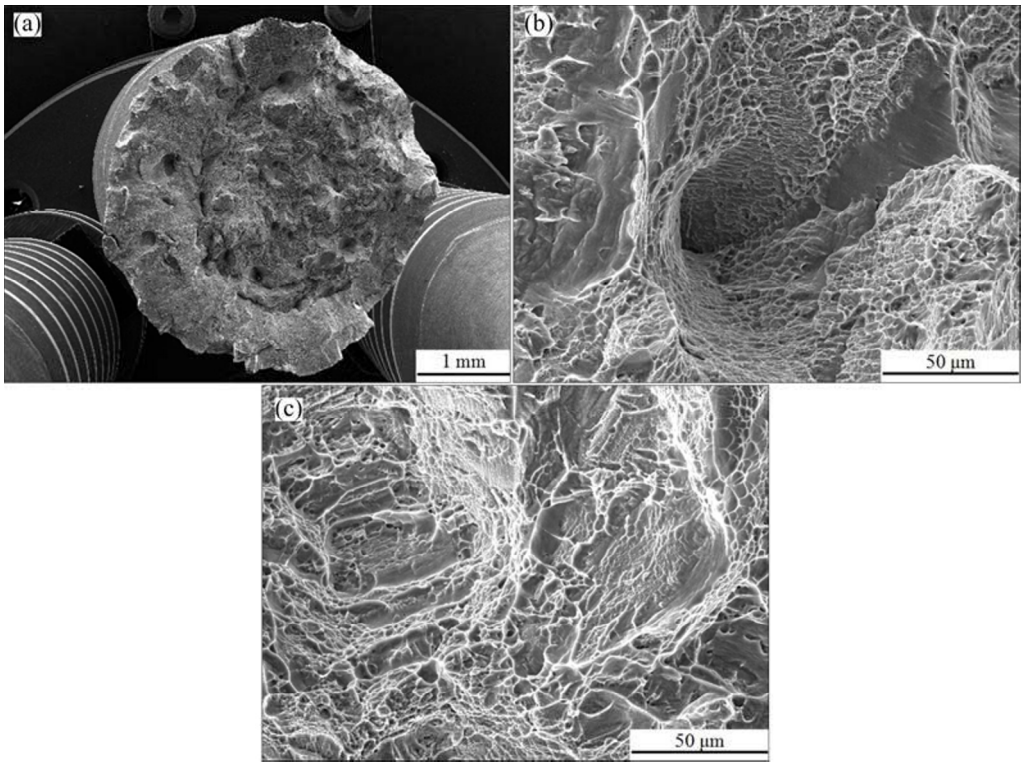

Fig. 7 Fractured morphology of heat-treated Ti−5Al−2Sn−2Zr−4Mo−4Cr specimens with Widmanstätten microstructure (a) and corresponding magnification image (b) and cleavage plane and shallow dimples (c)

ductility. The appearance of cleavage plane is unnegligible, and the intercrystalline fractured mechanism also causes a decrease in ductility. Thus, small shrinkage, large and deep cracks, small and shallow dimples on the fractured surfaces prove low ductility of Widmanstätten microstructure [22].

4 Conclusions

1) For obtaining the equiaxed, bi-modal and Widmanstätten microstructures, the heat treatment temperatures of Ti−5Al−2Sn−2Zr−4Mo−4Cr followed by FC at a holding time of 30 min are 830, 890 and 920 °C, respectively.

2) As the heating temperature increases from 830 to 890 °C followed by FC, the volume fraction of primary α phase of Ti−5Al−2Sn−2Zr−4Mo−4Cr decreases from 45.8% to 15.5%, and disappears at 920 °C. The amount and width of the secondary α phase increase with the increase of heating temperature. Compared with AC, FC promotes the precipitation of secondary α phase and the growth of α phase.

3) Both equiaxed and bi-modal microstructures of Ti−5Al−2Sn−2Zr−4Mo−4Cr exhibit high strength and ductility, and the YS, RA and El for Widmanstätten microstructure are low. However, the UTS for Widmanstätten microstructure is higher than that for other microstructures.

4) The fractured surface morphologies for the equiaxed and bi-modal microstructures of Ti−5Al−2Sn−2Zr−4Mo−4Cr in room temperature tension show the dimple fractured mechanism with good ductility, and that for the Widmanstätten microstructure shows the intercrystalline and dimple fractured mechanism contemporarily with poor ductility.

References

[1] MAJUMDAR P. Effects of heat treatment on evolution of microstructure of boron free and boron containing biomedical Ti−13Zr−13Nb alloys [J]. Micron, 2012, 43: 879−886.

[2] LEYENS C, PETERS M. Titanium and titanium alloys: Fundamentals and applications [M]. New York: Wiley-VCH, 2003: 16−18.

[3] IVASISHIN O M, MARKOVSKY P E, MATVIYCHUK Y V, SEMIATIN S L, WARD C H, FOX S. A comparative study of the mechanical properties of high-strength β-titanium alloys [J]. Journal of Alloys and Compounds, 2008, 457: 296−309.

[4] MARKOVSKYA P E, SEMIATIN S L. Microstructure and mechanical properties of commercial-purity titanium after rapid (induction) heat treatment [J]. Journal of Materials Processing Technology, 2010, 210: 518−528.

[5] SIENIAWSKI J, FILIP R, ZIAJA W. The effect of microstructure on the mechanical properties of two-phase titanium alloys [J]. Materials and Design, 1997, 18(4−6): 361−363.

[6] FILIP R, KUBIAK K, ZIAJA W, SEINIAWSKI J. The effect of microstructure on the mechanical properties of two-phase titanium alloys [J]. Journal of Materials Processing Technology, 2003, 133: 84−89.

[7] FROES F H. Encyclopedia of materials: Science and Technology [M]. Oxford: Pergamon Press, 2001: 9361−9364.

[8] LÜTJERING G. Influence of processing on microstructure and mechanical properties of (α+β) titanium alloys [J]. Materials Science and Engineering A, 1998, 243: 32−45.

[9] SHI Zhi-feng, GUO Hong-zhen, HAN Jin-yang, YAO Ze-kun. Microstructure and mechanical properties of TC21 titanium alloy after heat treatment [J]. Transactions of Nonferrous Metals Society of China, 2013, 23(10): 2882−2889.

[10] BOYER R, WELSCH G, COLLINGS E W. Materials properties handbook: Titanium alloys [M]. Ohio: ASM, 1994: 453−463.

[11] SEMIATIN S L, KNISLEY S L, FAGIN P N, BARKER D R, ZHANG F. Microstructure evolution during alpha-beta heat treatment of Ti−6Al−4V [J]. Metallurgical and Materials Transactions A, 2003, 34: 2377−2386.

[12] LI H, LI M Q, HAN T, LIU H B. The deformation behavior of isothermally compressed Ti-17 titanium alloy in α+β field [J]. Materials Science and Engineering A, 2012, 546: 40−45.

[13] MU Z, LI H, LI M Q. The microstructure evolution in the isothermal compression of Ti-17 alloy [J]. Materials Science and Engineering A, 2013, 582: 108−116.

[14] TARÍN P, FERNÍANDEZ A L, SIMÓN A G, BADIA J M, PIRIS N M. Transformations in the Ti−5Al−2Sn−2Zr−4Mo−4Cr (Ti-17) alloy and mechanical and microstructural characteristics [J]. Materials Science and Engineering A, 2006, 438−440: 364−368.

[15] TEIXEIRA J D C, APPOLAIRE B, AEBY-GAUTIER E, DENIS S, CAILLETAUD G, SPÄTH N. Transformation kinetics and microstructures of Ti-17 titanium alloy during continuous cooling [J]. Materials Science and Engineering A, 2007, 448: 135−145.

[16] WANG K, LI M Q. Morphology and crystallographic orientation of the secondary α phase in a compressed α/β titanium alloy [J]. Scripta Materialia, 2013, 68: 64−967.

[17] IBRAHIM K M, EL-HAKEEM A M, ELSHAER R N. Microstructure and mechanical properties of cast and heat treated Ti−6.55Al−3.41Mo−1.77Zr alloy [J]. Transactions of Nonferrous Metals Society of China, 2013, 23(12): 3517−3524.

[18] DEHGHAN-MANSHADI A, REID M H, DIPPENAAR R J. Effect of microstructural morphology on the mechanical properties of titanium alloys [J]. Journal of Physics: Conference Series, 2010, 240: 1−5.

[19] WANG Xiao-yan, LIU Jian-rong, LEI Jia-feng, CAO Ming-zhou, LIU Yu-yin. Effects of primary and secondary α phase on tensile property and fracture toughness of Ti-1023 alloy [J]. Acta Metallurgica Sinica, 2007, 43: 1129−1137.

[20] GIL F J, GINEBRA M P, MANERO J M, PLANELL J A. Formation of α-Widmanstätten microstructure: Effects of grain size and cooling rate on the Widmanstätten morphologies and on the mechanical properties in Ti6Al4V alloy [J]. Journal of Alloys and Compounds, 2001, 329: 142−152.

[21] PETERS J O, LÜTJERING G. Comparison of the fatigue and fracture of α+β and β titanium alloys [J]. Metallurgical Materials Transactions A, 2001, 32: 2805−2818.

[22] HUANG D M, WANG H L, CHEN Y, GUO H. Influence of forging process on microstructure and mechanical properties of large section Ti−6.5Al−1Mo−1V−2Zr alloy bars [J]. Transactions of Nonferrous Metals Society of China, 2013, 23(8): 2276−2282.

热处理 Ti−5Al−2Sn−2Zr−4Mo−4Cr 合金的显微组织与力学性能

李慧敏，李淼泉，罗 皎，王 柯

西北工业大学 材料学院，西安 710072

摘 要：研究热处理参数对 Ti−5Al−2Sn−2Zr−4Mo−4Cr 合金显微组织的影响及其等轴组织、双态组织和魏氏组织的室温拉伸力学性能和拉伸断口形貌。获得 3 种典型显微组织的热处理温度分别为 830、890 和 920 ℃，并保温 30 min 后炉冷。炉冷时，初生 α 相体积分数随热处理温度的升高而减小，在热处理温度为 830、890 和 920 ℃ 时，初生 α 相的体积分数分别为 45.8%、15.5%和 0；空冷时，初生 α 相体积分数的变化规律类似。升高热处理温度和炉冷均有利于次生 α 相的析出和长大。等轴组织具有良好的综合拉伸性能，其抗拉强度、屈服强度、伸长率及断面收缩率分别为 1035 MPa、1011 MPa、20.8%和 58.7%；双态组织的屈服强度和伸长率略低于等轴组织的屈服强度和伸长率；魏氏组织的韧性差、屈服强度低，但抗拉强度高达 1078 MPa。等轴组织和双态组织的室温拉伸断口呈韧窝断裂，塑性较好；魏氏组织的室温拉伸断口中韧窝断裂和晶间断裂共存，塑性较差。

关键词：钛合金；热处理；显微组织；力学性能；断口形貌

(Edited by Wei-ping CHEN)